MATERIALS CHEMISTRY
FRONTIERS

RESEARCH ARTICLE

View Article Online
View Journal

Cite this: DOI: 10.1039/d0qm00006j

The pressing-induced formation of a large-area supramolecular film for oil capture†

Wenkai Wang, Mengqi Xie, Hongjun Jin, Wanwan Zhi, Kaerdun Liu, Cheng Ma, Peilong Liao, Jianbin Huang and Yun Yan *

The ability to quickly and efficiently capture oil from diverse bodies of water is very important for environmental considerations. Here, we report a supramolecular film that displayed quick oil adsorption, specifically within minutes, with this film fabricated by carrying out a pressing of precipitates formed from commercially available poly(sodium 4-styrenesulfonate) (PSS) and oppositely charged dimethyldi-tetradecylammonium bromide (DTTAB). Under mechanical pressure, the DTTAB molecules were found to form large lamellar mesophases with sizes comparable to the wavelength of visible light. These mesophases were further connected electrostatically *via* PSS chains into the bulk film. Oils could be captured by the hydrophobic mesophases in the film owing to the effect of the "like likes like" principle. This effect, being independent of pore size, afforded the complete adsorption of oil within minutes in water samples ranging from dilute water to saline water. Oil recovery was carried out here using a desorption process, and the desorbed film could be reused. Furthermore, the film was regenerated under mechanical pressure after being damaged. Mass-scale fabrication of the film was shown to be possible using a household noodle machine. All these features make the present film a competitive oil adsorption material that can be extended to future industrial production.

Received 8th January 2020,
Accepted 26th March 2020

DOI: 10.1039/d0qm00006j

rsc.li/frontiers-materials

Introduction

Water pollution has become the most serious threat to the lives of organisms at various positions of ecological chains, leading to catastrophic results for human beings. Oil and organic chemical spillages are the primary origins of water pollution.[1,2] To remove these pollutants from water, effective but economic adsorbents are highly desired. Conventional adsorbents, such as activated carbon,[3] natural fiber,[4] and zeolite,[5] suffer from several problems, such as low adsorption capacity, non-recyclability, or the need to consume energy sources to regenerate them using current processes. To tackle these problems, many efforts have been devoted to developing advanced adsorbents.[6–14] Heretofore, several extraordinary materials have been fabricated, such as boron nitride nanosheets,[8] graphene-based aerogels/sponges,[11,15–21] and carbon nanotube (CNT)-based aerogels/sponges.[22–24] However, they are expensive and their preparation conditions are harsh, which prevent their scaled-up production and practical application.[25] Adsorbents that are inexpensive, easy to prepare, renewable, and amenable to scaled-up production would, of course, be more promising than their counterparts made using complicated procedures.

Efficient adsorption of oil requires the adsorbents to have large specific surface areas.[25,26] In this regard, porous and film/membrane materials are inherently advantageous.[10,26,27] Compared to porous materials that are often made with complicated chemistries, films can be generated much more easily. For instance, a recent study in our group revealed that large-area self-supporting thin films can be made by pressing supramolecular precipitates.[28,29] We have therefore expected to be able to generate films using a similar strategy to collect oil. To this end, we have focused our attention on the precipitates formed from commercially available polyelectrolytes and oppositely charged surfactants. Precipitates formed from polyelectrolytes and oppositely charged surfactants have been reported to form various types of films when cast from organic solutions.[30]

Beijing National Laboratory for Molecular Sciences (BNLMS), College of Chemistry and Molecular Engineering, Peking University, Beijing 100871, China.
E-mail: yunyan@pku.edu.cn

† Electronic supplementary information (ESI) available: The elemental analysis results for the DTTAB-PSS film, a TEM image of the DDTAB vesicles, DLS data of a 20 mM DTTAB solution, optical images of the processes used to prepare the DTTAB–PSS film materials, TGA curves for the dry and wet DTTAB–PSS films, 2D GIXRD patterns for the DTTAB–PSS film, chemical structure and model of the DTTAB molecule, an SEM image of the surface of the DTTAB-PSS film, an SEM image of a cross section of the DTTAB–PSS film, XRD patterns of the DTTAB–PSS film before adsorption, after adsorption and after regeneration for different organic solvents, a schematic diagram of the recycling of the film for petroleum adsorption in DI water, a schematic diagram of the recycling of the film for petroleum adsorption in 150 mM NaCl solution and dirty water, photographs of the DTTAB–PSS film after it was immersed in DI water and in a 33 wt% NaCl solution for 72 h, and a DSC trace of the PSS–DTTAB film. See DOI: 10.1039/d0qm00006j

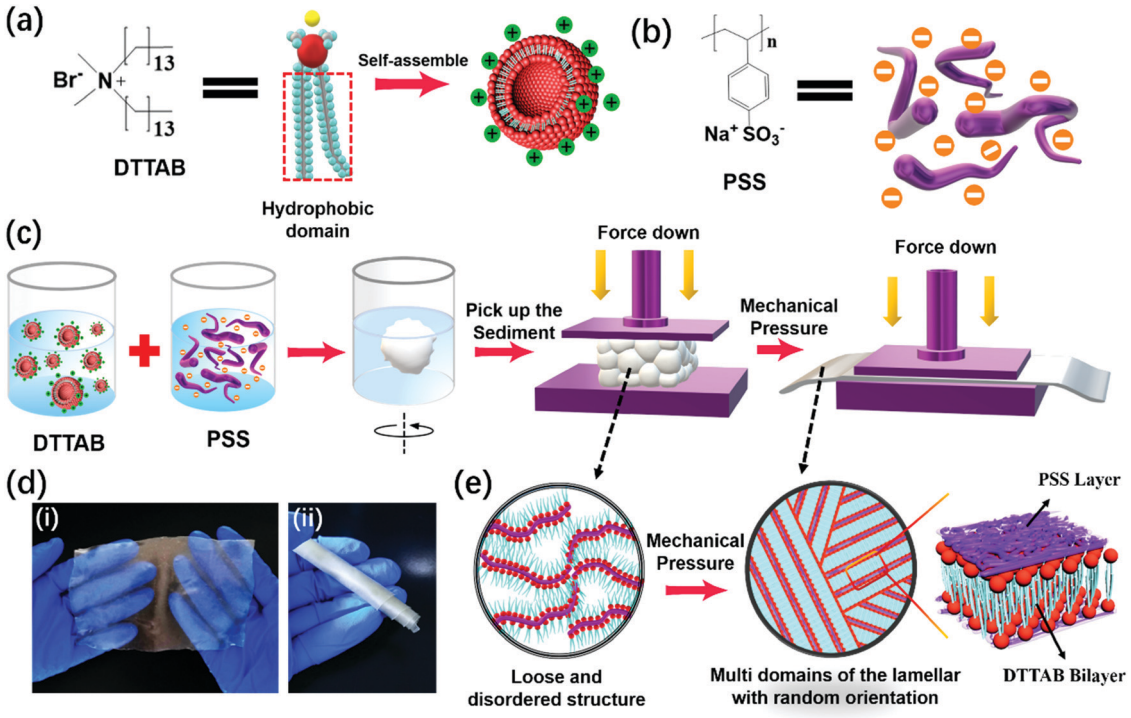

Fig. 1 (a) The chemical structure of DTTAB and an illustration of the self-assembly of DTTAB into vesicles. (b) The chemical structure of PSS. (c) A schematic illustration of the process used to generate DTTAB–PSS films. This process involved mixing the aqueous solutions of oppositely charged DTTAB vesicles and PSS, and then directly pressing the generated white precipitates into a transparent plastic film under ambient conditions. (d) Mass-scale fabrication of the DTTAB–PSS film: (i) a photograph of a flexible film with dimensions of 150 mm × 80 mm × 0.3 mm and (ii) a photograph of a rolled 150 mm × 80 mm × 0.3 mm film. (e) Schematic illustrations of the lamellar structure formed from PSS and DTAB after the application of mechanical pressure.

We supposed that pressing the fresh precipitates would also lead to the formation of supramolecular films owing to the fusion of the surfactant domains under mechanical pressure. In the meantime, the surfactant domains in the film would be expected to serve as reservoirs for oil in the process of oil recovery. However, this hypothesis has not yet been tested.

In this work, we showed that pressing the precipitates formed from the commercially available poly(sodium 4-styrenesulfonate) (PSS) and the oppositely charged vesicle-forming surfactant ditetradecylammonium bromide (DTTAB) (Fig. 1a and b) can indeed lead to the formation of supramolecular films (Fig. 1) capable of adsorbing oils from both fresh and salty water. In contrast to the case for the simple condensing of small particles in powder materials, the mechanical pressure facilitated the formation of large lamellar domains of DTTAB when the precipitates were pressed, a result that indicated the generation of supramolecular materials from the amorphous precipitates. Since the film was formed by pressing the PSS–surfactant precipitates with mild mechanical pressure, any damaged film could be regenerated or mended under the same pressure; and reuse of the film was shown to be possible after the oil was recovered. Compared to strategies previously reported for various oil adsorbents, the current strategy involved only room-temperature physical production techniques in aqueous conditions with commercially available materials; and mass-scale fabrication of the film was found to be possible using a household noodle machine, a process amenable to advancing the key goal of global sustainability.

Results and discussion

Synthesis and basic characterizations of the thin films

The commercially available ditetradecylammonium bromide (DTTAB) and poly(sodium 4-styrenesulfonate) (PSS) were chosen as the oppositely charged pair of polyelectrolyte and surfactant (Fig. 1a and b). DTTAB can, at appropriate concentrations, self-assemble into vesicles in water.[31] The vesicle membrane is composed of tail-to-tail-arranged DTTAB bilayers,[32,33] which provide a sufficiently hydrophobic environment for oil adsorption (Fig. 1e). In the current study, a TEM observation revealed the diameter of the dried vesicles to range from 50 to 200 nm (Fig. S1a, ESI†), whereas dynamic light scattering (DLS) measurement suggested much larger *in situ* dimensions of these vesicles of about 400 nm (Fig. S1b, ESI†). The scattering of light by these large vesicles endowed the aqueous DTTAB system with a bluish hue (Fig. S2, ESI†). After adding the PSS solution to the vesicular DTTAB system, white flocculates formed as the charge of the system reached a balance (Fig. S2, ESI†). Amazingly, the fresh white flocculates could be finger pressed into a whitish film under mechanical pressures greater than 5 MPa, and this film gradually became transparent within

30 min (Fig. 1c and Fig. S2, ESI†). By comparing the weight of the film with those of the solid PSS and DTTAB materials, the yield of the film was estimated to be 75%. Elemental analysis revealed that the film was a charge-neutral product composed of the polystyrene sulphate polyanions and ditetradecyl ammonium cations (Table S1, ESI†), but thermal gravimetric analysis (TGA) suggested that each pair of the oppositely charged unit contained two bound water molecules (Fig. S3, ESI†). Differential scanning calorimetry (DSC) measurements revealed an endothermic peak at −30.8 °C in the cooling process and exothermic peak at −25.5 °C in the heating process, but no phase transition in the temperature range of 0–200 °C (Fig. S4, ESI†). This result indicated that the DTTAB chain melted at temperatures below 25 °C, but remained in a stable liquid crystalline state in the broad temperature range of 0–200 °C, a set of features ensuring their further application as stable film materials. Hydration of the ion pairs of PSS and DTTAB with very tightly bound water molecules may have provided the major contribution to the plasticization of the DTTAB–PSS film.[34]

The structure of the film was further analyzed with X-ray diffraction (XRD) (Fig. 2a). Three Bragg diffraction peaks, corresponding to distances of 32.1 Å, 16.1 Å and 10.7 Å, were observed; these peaks indicated the presence of lamellar structures.[35] The thickness of the lamellae was determined from the 001 diffraction peak to be 32.1 Å, *i.e.*, approximately two times the length of an extended DTTAB molecule (Fig. S5, ESI†). This result indicated that the DTTAB molecules assembled into bilayers in the film. The oppositely charged PSS chains were thus expected to fold in between the bilayers to neutralize the charges on the ammonium heads of DTTAB. Two-dimensional grazing incidence X-ray diffraction (2D GIXRD) measurements revealed a strong ring for the 001 diffraction, but a weak arch for the 002 diffraction, indicating a random orientation of the DTTAB bilayers[36] (Fig. 2b and Fig. S6, ESI†). In line with this conclusion, colored birefringence of the film was observed under a polarized optical microscope (POM) (Fig. 2c). Strong extinction occurred as the sample in between two vertically oriented polarizers were aligned at angles of 0, 90, 180 and 270 degrees relative to the polarizers, whereas the brightest birefringence was observed when these angles were 45, 135, 225 and 315 degrees, indicating the presence of large area of ordered liquid crystalline mesophases in the film.[37]

An SEM image of a cross section of the film, shown in Fig. 2d, further confirmed the formation of lamellar structures in the film. In this image, the morphology of the cross section of the film was observed to be very coarse, which probably was due to the apparent random orientation of the bilayers. Furthermore, the large sizes of the bilayer domains were confirmed in the SEM image as well. Some parallel ridges were observed, and they were apparently cross sections of bilayers vertical to the cut. The bilayer lamellae were observed to have dimensions of up to several micrometers (Fig. 2d), much larger than the wavelength of visible light. This observation was consistent with the film having displayed evident birefringence under a polarized optical microscope (POM) (Fig. 2c).

Because the DTTAB–PSS film was formed by pressing the fresh precipitates with a mechanical force, it could—regardless

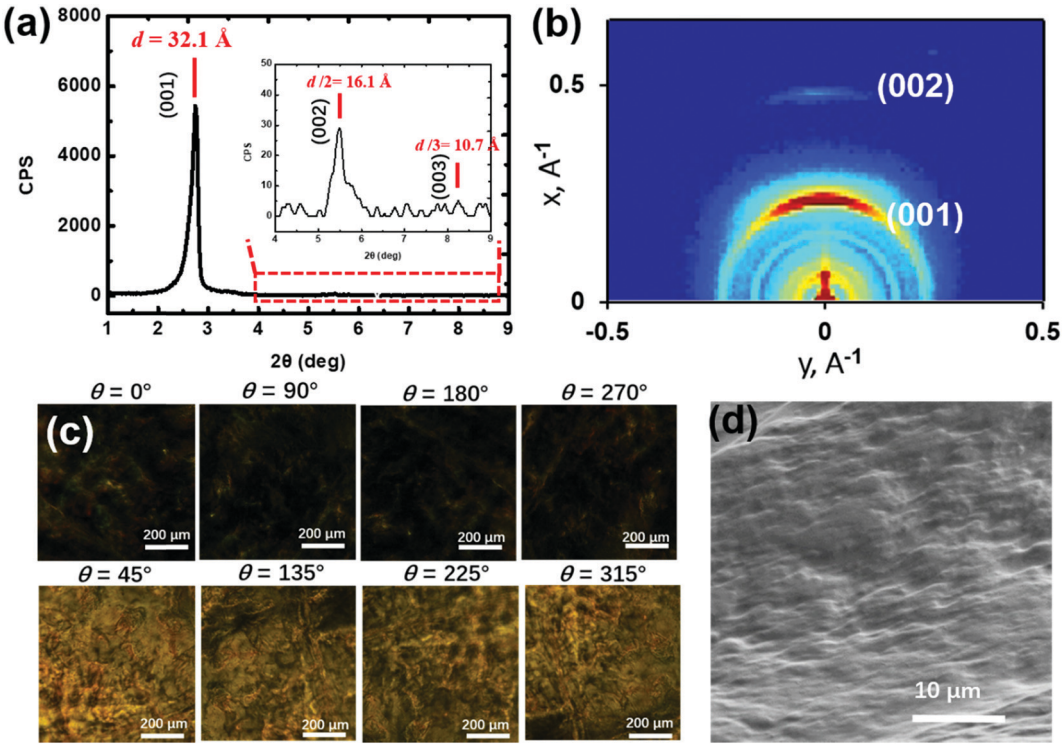

Fig. 2 (a) The XRD pattern of the DTTAB–PSS film. (b) The 2D GIXRD pattern of the DTTAB–PSS film. (c) POM images of the transparent DTTAB–PSS film aligned at various angles relative to two surrounding vertically arranged polarizers. (d) SEM image of a cross section of the DTTAB–PSS film.

of what damage it incurred—be regenerated again and again under the same mechanical pressure after being wetted with water. As shown in Fig. 3a, after wetting the film with water drops, the fragments of the film could be quickly kneaded together. Pressing the kneaded complex by hand over a glass or using a household noodle machine (Fig. 3b) led to the production of a new DTTAB–PSS film. Compared with the originally made film, the regenerated DTTAB–PSS film showed no detectable loss of mass and maintained the original transparency. The film could be made as thin as about 20 μm (Fig. S7, ESI†) using finger pressure. Meanwhile, mechanical tests showed that the regenerated DTTAB–PSS film retained the mechanical properties of the original one (Fig. 3c). In particular, its toughness remained constant in the range 100–115 kJ m^{-3} (Fig. 3d). This property manifested itself in nearly unchanged energies and structures of the film for successive remolding cycles during plastic deformation.[38] Carrying out the recycling test dozens of times did not noticeably change the mechanical properties of the film (Fig. 3c). This result indicated the ability to engineer an excellently reversible DTTAB–PSS film.

Removal of petroleum and organic solvent from water surfaces

The film, due to its being full of hydrophobic domains formed by DTTAB, was expected to have an inherent ability to adsorb oil and organic chemicals from water as a result of the "like likes like" principle. As shown in Fig. 4a, in the presence of the film, floating oil was adsorbed rapidly, specifically within minutes. The oil adsorption rate was not noticeably influenced by the thickness of the film: films with different thicknesses, specifically 0.30 mm, 0.46 mm, 1.22 mm, 1.69 mm, and 2.51 mm, respectively, were made using a household noodle machine, with the different thickness resulting from adjusting the distance between the two rollers of the machine; and the relative adsorption capacities of these five films toward petroleum each reached about 50% within the initial 10 seconds, and then 100% within 5 minutes (Fig. 4b). We supposed that in the initial 10 seconds, the petroleum was quickly captured by the hydrophobic domains in the film *via* the "like likes like" mechanism, whereas the oil capture rate then decreased with time due to a reduction in the relative number of unoccupied hydrophobic domains.

It should be mentioned, however, that the relative adsorption capacity did decrease with increasing film thickness (Fig. S8, ESI†). As the thickness of the film was increased from 0.3 mm to 2.51 mm, the weight of the adsorbed petroleum dropped from 220% of the film to below 50%. This result indicated that it was difficult for the petroleum to diffuse into the film as the thickness of the film was increased. Consequently, for practical considerations, we suggest use of 0.3 mm-thick films. Although it was possible to obtain even thinner films, they were found to be not as durable in terms of mechanical damage.

After adsorbing petroleum, the saturated DTTAB–PSS film still floated on the water surface (Fig. 4a), which indicated that the film would be easy to collect and remove. It was very exciting to discover the ability to simply apply petroleum ether

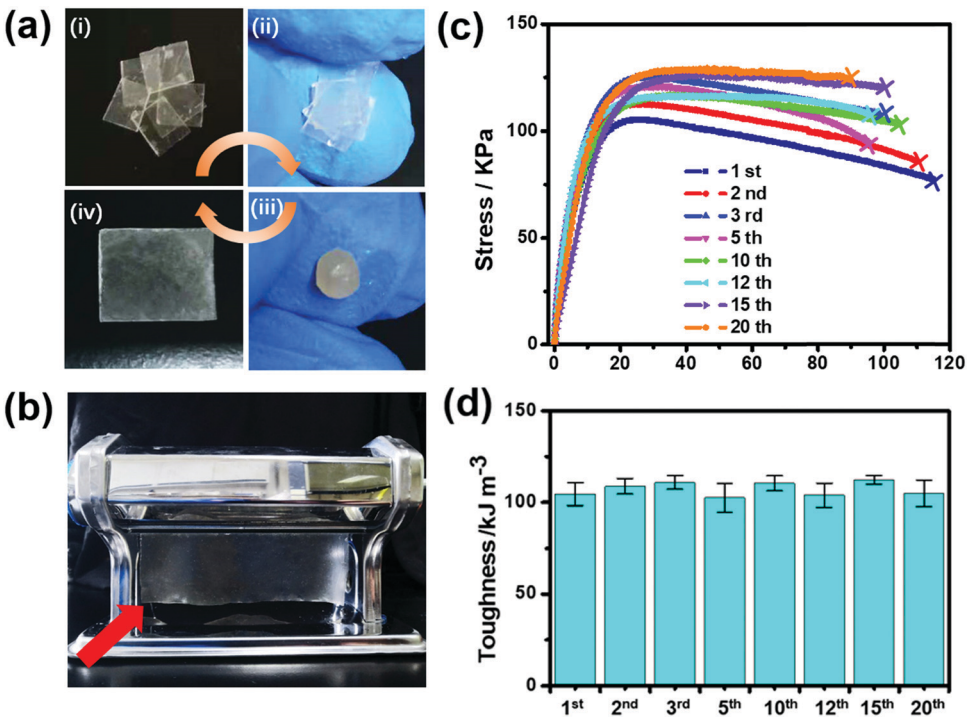

Fig. 3 (a) The procedure used to regenerate the film. (b) The large-scale production of the DTTAB–PSS film using a household noodle machine. (c) Stress–strain curves of the DTTAB–PSS films subjected to different numbers of cycles of remolding. (d) Toughness values of the original and regenerated films.

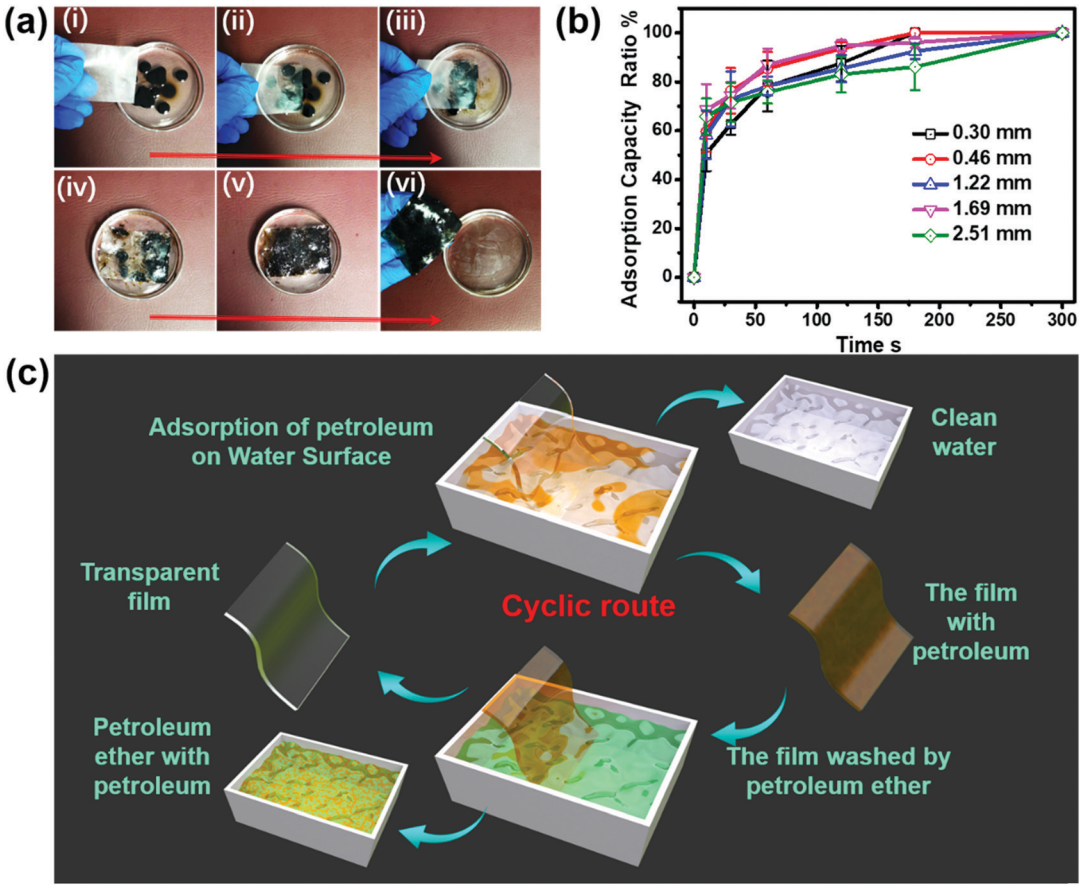

Fig. 4 (a) Photographs of the oil adsorption process using the DTTAB–PSS film with a thickness of 0.30 mm. (b) Relative adsorption capacities of DTTAB–PSS films of different thicknesses to adsorb petroleum. (c) A schematic diagram of the procedure used to recycle the film for petroleum adsorption.

to wash off this physically adsorbed petroleum, and to then reuse the desorbed film (Fig. 4c and Fig. S9, ESI†). The reused film did exhibit a slight yellowish color (Fig. S9, ESI†), due to the presence of residual oil in the film.

XRD measurements revealed that the 001 diffraction peak, for example, shifted to a lower angle after the petroleum adsorption, yet moved back towards the higher angle after the desorption, although not quite to its original position (Fig. 5a). This result confirmed that the adsorbed oil was hosted in the bilayers of DTTAB, and that after desorption there was still some residual oil in the film. As shown in Fig. 5c, the amount of petroleum adsorbed by the fresh 0.3 mm-thick DTTAB–PSS film was 220 wt% of its weight, whereas the adsorption capacity of the film decreased when the film was repeatedly used for another cycle of oil recovery. Nevertheless, the petroleum adsorption capacity of the DTTAB–PSS film was still 121.7% after ten cycles of reuse. The maximum swelling rate in pure water (*i.e.*, the weight ratio of the water taken up) was 19.6% within 72 h. This result indicated that the film was still able to adsorb a mass of petroleum comparable to its own mass. Many oil-capturing materials have been shown to be capable of capturing oil with masses over ten times their own respective masses.[39] However, most of these materials require expensive and energy-consuming fabrication processes, and can hardly be regenerated. In contrast, the current film was generated in an extremely economical manner and found to display excellent rejuvenability and reusability.

In most cases, oil spillage occurs in the sea. Therefore, it is very relevant to test the oil-adsorbing ability of a film in salty water. To this end, the fresh water was replaced by a 33% NaCl solution. Amazingly, in this condition the initial oil capture ability was 237.1%, *i.e.*, 8.2% better than that in fresh water (220.0%) (Fig. 5c). This enhanced oil-capturing ability was attributed to the unique ionic interaction between DTTAB and PSS. Because the ionic interaction can be shielded by NaCl,[40] the molecular packing in the film would become looser in a salt solution. As a result, the oil molecules could more easily enter the film, so that the hydrophobic domains can be better utilized. It is worth noting that the oil recovery in salty water was also found to be more complete than in fresh water. As shown in Fig. 5b, the 001 diffraction peak for the film after desorption of oil occurred nearly at the same position as in the original film, indicating that the slightly weaker ionic interaction between PSS and DDTAB would be beneficial for capturing oil in the sea. Strikingly, the film according to our measurements was not be damaged by salty water (Fig. 5b and Fig. S10, ESI†), with

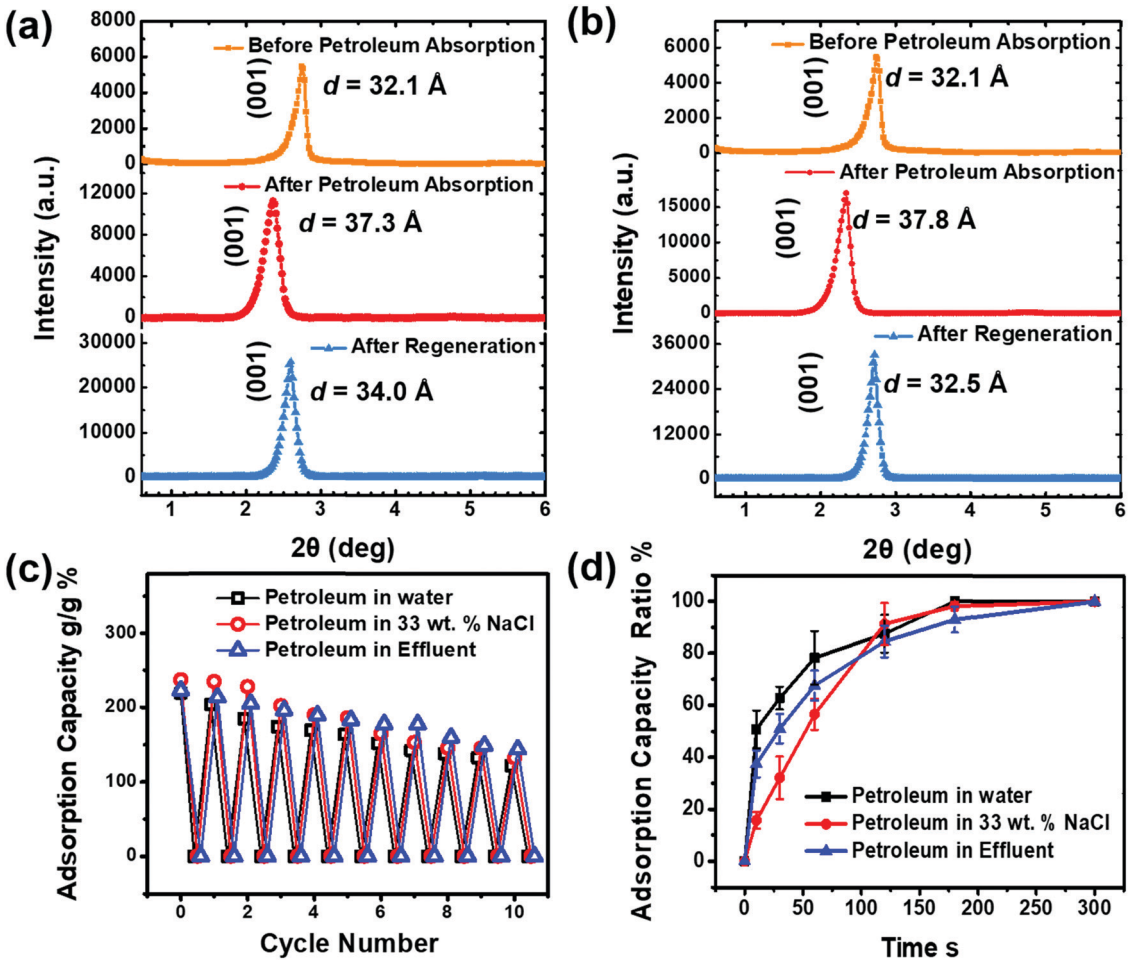

Fig. 5 (a and b) XRD patterns of the DTTAB–PSS film before it was used to adsorb petroleum, after it was used to adsorb petroleum, and after it was regenerated in (a) DI water and (b) 33 wt% NaCl solution. (c) Recycling test of the adsorption capacities of the DTTAB–PSS film for petroleum in DI water, 33 wt% NaCl solution, and dirty water containing much dust, respectively. Ten cycles were tested. (d) The petroleum adsorption efficiency of the DTTAB–PSS film in DI water, 33 wt% NaCl solution, and dirty water containing much dust, respectively. The thickness of the film was 0.3 mm.

this lack of damage attributed to the oil adsorption process being so quick that it completed within a couple of minutes. The film was in fact found to remain stable in salty water for 72 hours (Fig. S11, ESI†). Furthermore, our results indicated that the film adsorbents tolerated dirty water that contained much dust (Fig. S12, ESI†). Also, no noticeable effect of any adsorption of dust by the film surface on the efficiency of oil recovery was expected due to the "like likes like" mechanism of the oil capture. As shown in Fig. 5c, the recycling ability of the film in dirty water was indeed the same as that in clean water. This result indicated that the dust did not block the oil adsorption pathways in the film. Thus, the present film displayed a distinct advantage in practical application over those porous materials that can be deactivated in dirty water.

The oil capture results of the film for another nine water pollutants including alkanes (cyclohexane, *n*-pentane, *n*-octane), alcohols (2-propanol, octanol), aromatic compounds (benzene, toluene) and major substances of petrochemical–carbon 9 (mesitylene, indene) were investigated (Fig. 6a and b). The film was found to be capable of adsorbing all of the tested chemicals (Fig. 6a, b and Fig. S13, ESI†). Finally, guided oil capture was shown to be possible by doping magnetic Fe_3O_4 nanoparticles into the film. The special film formation process allowed the loading of magnet nanoparticles in the film facilely by coprecipitating the nanoparticles into the film. As the suspension of Fe_3O_4 nanoparticles was previously added to PSS or DTTAB solution, the Fe_3O_4 nanoparticles could be doped into the film. As a result, the DTTAB–PSS film could be made to move in a specified direction under the control of an external magnet (Fig. 6c). Moreover, a slightly remote guiding of the film was shown to be possible (Fig. 6d), a feature that would provide practical convenience to collecting any residual oil in gaps difficult to reach with the film.

Conclusions

In summary, we developed an inexpensive facile physical approach, involving pressing the precipitates formed from polystyrene sodium sulphate and DTTAB, to generate a supramolecular film that was shown to be usable for capturing

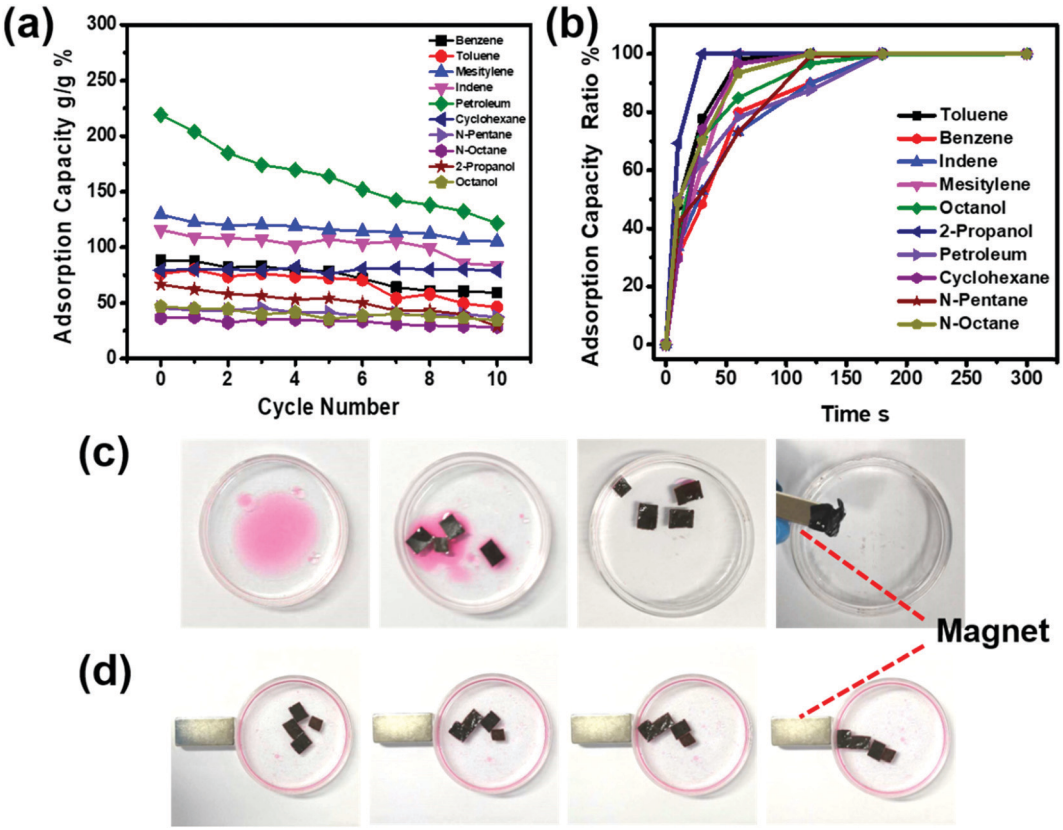

Fig. 6 (a) Recycling test of the adsorption capacities of the DTTAB–PSS film for petroleum and other organics. Ten cycles were tested. (b) Efficiency curves for the adsorption of petroleum and organic solvents by DTTAB–PSS films. (c and d) The magnetically driven removal of mesitylene, which was dyed using Oil Red O, from the surface of water. As shown in panel (d), remote magnetic removal of the film was found to be possible.

spilled oil in water. The film was composed of hydrophobic bilayers, which can adsorb spilled oil within minutes from both fresh and salty water *via* a 'like likes like' mechanism. This mechanism apparently avoided the blocking of pores suffered by many porous materials, and thus allowed for good practical applications of the film in natural dirty water systems. Compared with other adsorbents, the developed film displayed rapid and efficient adsorption and high reusability and recyclability, features that are important for achieving energy savings. It is noteworthy that the thin films developed in this work provide a new material platform for the development of special and customizable film materials on the micro- and macro-scales, which opens up opportunities for advanced applications for the multifunctional operation of films.

Experimental

Preparation of the DTTAB–PSS film

Dimethylditetradecylammonium bromide (DTTAB) and sodium polystyrene sulfonate (PSS, $M_w \sim 70\,000$) were purchased from the Sigma-Aldrich Corporation. All other reagents were of AR grade. An aqueous solution of DTTAB and an aqueous solution of PSS were combined in such a manner so as to yield final concentrations of 20 mM for the sulfonate negative charges of PSS and 20 mM for the ammonium positive charges of DTTAB. White precipitates immediately formed after these components were mixed, and they were separated from the suspensions by subjecting the mixture to centrifugation at a speed of 10 000 rpm for 5 min. The collected precipitates were then treated in two parallel ways: (1) subjected to a pressure imposed by finger pressing and (2) household noodle machine manufacturing under an ambient environment. The household noodle machine used was a "Baijie Noodle Machine". It contained two stainless steel rollers, and the gap between them could be varied from 0.3 mm to 3 mm. By loading the pre-collected precipitates in the gap, the film was obtained as the machine was switched on, where the two rollers rotated in opposite directions. The thickness of the film was controlled by setting the width of the gap.

The yield of the DTTAB–PSS film (Y) was calculated using the equation $Y = M_d/(M_{PSS} + M_{DTTAB}) \times 100\%$, where M_d denotes the mass of the dried PSS-DTTAB film, M_{PSS} the mass of the PSS added, and M_{DTTAB} the mass of the DTTAB added. To test the H_2O swelling capability of the DTTAB–PSS film, the film was first weighed at its dry state, *i.e.*, its dry weight (W_d) was determined. Then it was immersed in DI water at a constant temperature of 20 °C for 72 h and the wet weight (W_w) was assessed after the removal of extra water with the help of a tissue. The mass swelling ratio (Q) was calculated using the equation $Q = (W_w - W_d)/W_d \times 100\%$, where W_w denotes the

mass of the wet film sample and W_d the mass of the dried film sample.

Functionalized DTTAB–PSS film

To fabricate functional materials based on this kind of film, Fe_3O_4 was embedded into samples of the film by carrying out coprecipitation processes. The Fe_3O_4 nanoparticles were pre-dispersed in either the solution of polyelectrolyte or the solution of surfactant before mixing. After coprecipitation, the resultant precipitates were subjected to pressing, in order to fabricate the functional plastic films.

Damaging, remolding and rejuvenating of DTTAB–PSS Film

Films were cut into separate pieces either by using a razor blade or scissor. The pieces of such cut films were then brought together using hands or tweezers. After dropping water onto these pieces, they softened and could be remolded into any other desired shape. Under the load exerted by a noodle machine or human fingers, the softened materials could, for example, be re-molded into transparent films instantly without any cracks, and this process of re-juvenescence was carried out repeatedly many times without detectable fatigue in the mechanical properties of the film.

Petroleum removal and recycling tests

The adsorption capacity, W (wt/wt)%, values were obtained by measuring the mass of the dry DTTAB–PSS film, and then the mass after it was used to adsorb petroleum. For the oil adsorption efficiency test, a film was used to adsorb oil, and the oil adsorption mass (W_n) was recorded as a function of time. When the oil adsorption remained unchanged, 100% of the possible oil adsorption of the film was considered to have been achieved (W_{full}). Therefore, the oil adsorption efficiency of each time point was obtained using the formula $(W_n/W_{full}) \times 100\%$. For the recycling test, after the petroleum was adsorbed by the film on the water surface, the film was transferred into petroleum ether for washing for a few minutes. Then the resulting clean film was taken out, and from it a new film was constructed by following the above-described 'remolding and rejuvenating' method. The experiments on the relationship between film thickness and oil adsorption efficiency were carried out by preparing five films with different thicknesses (0.30 mm, 0.46 mm, 1.22 mm, 1.69 mm and 2.51 mm) using the household noodle machine, and then investigating their oil adsorption efficiencies, respectively.

Organic solvent removal and recycling tests

Nine different kinds of organic solvents were used in this study. The adsorption capacity, W (wt/wt)%, values were obtained by measuring the mass of the dry DTTAB–PSS film, and then the mass after solvent adsorption. For the recycling test, after the organic solvent was adsorbed by the film, the film was transferred to a vacuum drying chamber and left in there for 2 hours. The resulting clean film was then taken out, and used to constructed a new film by following the above-described 'remolding and rejuvenating' method.

Mechanical tests

The mechanical properties of the films were tested by using a WDW3020 electronic universal testing machine at room temperature. Stress–strain data were collected with a strain rate of 5 mm min^{-1}. All mechanical tests were conducted on dumbbell-shaped samples. Samples undergoing different numbers of remolding cycles of the same original film were used to measure the re-juvenescence ability of the materials; this ability was found to be outstanding.

Characterizations

Scanning electron microscopy (SEM) measurements were taken using a Hitachi S4800 microscope at an acceleration voltage of 1.0 kV. The films were placed on clean silicon wafers for SEM observations. X-ray diffraction (XRD) measurements were taken using a Rigaku Dmax-2400 diffractometer with Cu Kα radiation. The solid samples were placed on clean glass slides for small-angle range tests. Two-dimensional (2D) grazing incidence X-ray diffraction (GIXRD) patterns of the DTTAB–PSS film was obtained by using a Ganesha system (SAXSLAB, US) equipped with a multilayer focused Cu Kalpha radiation as the X-ray source (Genix 3D Cu ULD) and a semiconductor with LaB_6 for the wide-angle region and silver behenate for the small-angle region. A Linkam TST350 stage was used to study the evolution the structure with changing temperature. Regarding polarizing optical microscopy (POM) studies, photographs of birefringence were captured by using a LV100N polarizing microscope (Nikon Co.) at room temperature. Dynamic light scattering (DLS) measurements were taken using a NanoBrook NanoOmni instrument. All measurements were taken using DI water at 20 °C. Samples were photographed with θ ranging from 0° to 360°, where θ denotes the angle between the analyzer and the alignment direction of the sample. TGA experiments were carried out under nitrogen flow on a TA Instrument Q600 SDT at a heating rate of 10 °C min^{-1}. Differential scanning calorimetry (DSC) experiments were carried out under nitrogen using a TA Instrument Q2000 DSC at a heating rate of 10 °C min^{-1} with cycling between −80 °C to 220 °C.

Conflicts of interest

The authors declare no conflict of interest.

Acknowledgements

This work was financially supported by the National Natural Science Foundation of China (NSFC 91856120 and 21633002).

References

1 T. Dalton and D. Jin, Extent and frequency of vessel oil spills in US marine protected areas, *Mar. Pollut. Bull.*, 2010, **60**(11), 1939.

2 J. Aurell and B. K. Gullett, Aerostat Sampling of PCDD/PCDF Emissions from the Gulf Oil Spill In Situ Burns, *Environ. Sci. Technol.*, 2010, **44**(24), 9431.
3 A. Bayat, S. F. Aghamiri, A. Moheb and G. R. Vakili-Nezhaad, Oil spill cleanup from sea water by sorbent materials, *Chem. Eng. Technol.*, 2005, **28**(12), 1525.
4 G. Deschamps, H. Caruel, M.-E. Borredon, C. Bonnin and C. Vignoles, Oil Removal from Water by Selective Sorption on Hydrophobic Cotton Fibers. 1. Study of Sorption Properties and Comparison with Other Cotton Fiber-Based Sorbents, *Environ. Sci. Technol.*, 2003, **37**(5), 1013.
5 M. O. Adebajo, R. L. Frost, J. T. Kloprogge, O. Carmody and S. Kokot, Porous materials for oil spill cleanup: A review of synthesis and absorbing properties, *J. Porous Mater.*, 2003, **10**(3), 159.
6 P. Calcagnile, D. Fragouli, I. S. Bayer, G. C. Anyfantis, L. Martiradonna, P. D. Cozzoli, R. Cingolani and A. Athanassiou, Magnetically Driven Floating Foams for the Removal of Oil Contaminants from Water, *ACS Nano*, 2012, **6**(6), 5413.
7 X. Gui, Z. Zeng, Z. Lin, Q. Gan, R. Xiang, Y. Zhu, A. Cao and Z. Tang, Magnetic and Highly Recyclable Macroporous Carbon Nanotubes for Spilled Oil Sorption and Separation, *ACS Appl. Mater. Interfaces*, 2013, **5**(12), 5845.
8 W. Lei, D. Portehault, D. Liu, S. Qin and Y. Chen, Porous boron nitride nanosheets for effective water cleaning, *Nat. Commun.*, 2013, **4**, 1777.
9 J. Ge, H. Y. Zhao, H. W. Zhu, J. Huang, L. A. Shi and S. H. Yu, Advanced Sorbents for Oil-Spill Cleanup: Recent Advances and Future Perspectives, *Adv. Mater.*, 2016, **28**(47), 10459.
10 T. Li, L. Wang, K. Zhang, Y. Xu, X. Long, S. Gao, R. Li and Y. Yao, Freestanding Boron Nitride Nanosheet Films for Ultrafast Oil/Water Separation, *Small*, 2016, **12**(36), 4960.
11 J. Ge, L.-A. Shi, Y.-C. Wang, H.-Y. Zhao, H.-B. Yao, Y.-B. Zhu, Y. Zhang, H.-W. Zhu, H.-A. Wu and S.-H. Yu, Joule-heated graphene-wrapped sponge enables fast clean-up of viscous crude-oil spill, *Nat. Nanotechnol.*, 2017, **12**, 434.
12 M. Ge, C. Cao, J. Huang, X. Zhang, Y. Tang, X. Zhou, K. Zhang, Z. Chen and Y. Lai, Rational design of materials interface at nanoscale towards intelligent oil–water separation, *Nanoscale Horiz.*, 2018, **3**(3), 235.
13 J. Ge, F. Wang, X. Yin, J. Yu and B. Ding, Polybenzoxazine-Functionalized Melamine Sponges with Enhanced Selective Capillarity for Efficient Oil Spill Cleanup, *ACS Appl. Mater. Interfaces*, 2018, **10**(46), 40274.
14 Z. Lei, Y. Deng and C. Wang, Multiphase surface growth of hydrophobic ZIF-8 on melamine sponge for excellent oil/water separation and effective catalysis in a Knoevenagel reaction, *J. Mater. Chem. A*, 2018, **6**(7), 3258.
15 H.-P. Cong, X.-C. Ren, P. Wang and S.-H. Yu, Macroscopic Multifunctional Graphene-Based Hydrogels and Aerogels by a Metal Ion Induced Self-Assembly Process, *ACS Nano*, 2012, **6**(3), 2693.
16 K. Sohn, Y. Joo Na, H. Chang, K.-M. Roh, H. Dong Jang and J. Huang, Oil absorbing graphene capsules by capillary molding, *Chem. Commun.*, 2012, **48**(48), 5968.
17 H. Bi, X. Xie, K. Yin, Y. Zhou, S. Wan, R. S. Ruoff and L. Sun, Highly enhanced performance of spongy graphene as an oil sorbent, *J. Mater. Chem. A*, 2014, **2**(6), 1652.
18 R. Li, C. Chen, J. Li, L. Xu, G. Xiao and D. Yan, A facile approach to superhydrophobic and superoleophilic graphene/polymer aerogels, *J. Mater. Chem. A*, 2014, **2**(9), 3057.
19 J. Zou and F. Kim, Diffusion driven layer-by-layer assembly of graphene oxide nanosheets into porous three-dimensional macrostructures, *Nat. Commun.*, 2014, **5**, 5254.
20 Y. Luo, S. Jiang, Q. Xiao, C. Chen and B. Li, Highly reusable and superhydrophobic spongy graphene aerogels for efficient oil/water separation, *Sci. Rep.*, 2017, **7**(1), 7162.
21 H. Bi, X. Xie, K. Yin, Y. Zhou, S. Wan, L. He, F. Xu, F. Banhart, L. Sun and R. S. Ruoff, Spongy Graphene as a Highly Efficient and Recyclable Sorbent for Oils and Organic Solvents, *Adv. Funct. Mater.*, 2012, **22**(21), 4421.
22 M. B. Bryning, D. E. Milkie, M. F. Islam, L. A. Hough, J. M. Kikkawa and A. G. Yodh, Carbon Nanotube Aerogels, *Adv. Mater.*, 2007, **19**(5), 661.
23 X. Gui, J. Wei, K. Wang, A. Cao, H. Zhu, Y. Jia, Q. Shu and D. Wu, Carbon Nanotube Sponges, *Adv. Mater.*, 2010, **22**(5), 617.
24 R. Du, Q. Zhao, N. Zhang and J. Zhang, Macroscopic Carbon Nanotube-based 3D Monoliths, *Small*, 2015, **11**(27), 3263.
25 Q. Ma, H. Cheng, A. G. Fane, R. Wang and H. Zhang, Recent Development of Advanced Materials with Special Wettability for Selective Oil/Water Separation, *Small*, 2016, **12**(16), 2186.
26 R. K. Gupta, G. J. Dunderdale, M. W. England and A. Hozumi, Oil/water separation techniques: a review of recent progresses and future directions, *J. Mater. Chem. A*, 2017, **5**(31), 16025.
27 K. Jayaramulu, K. K. R. Datta, C. Rösler, M. Petr, M. Otyepka, R. Zboril and R. A. Fischer, Biomimetic Superhydrophobic/Superoleophilic Highly Fluorinated Graphene Oxide and ZIF-8 Composites for Oil–Water Separation, *Angew. Chem., Int. Ed.*, 2016, **55**(3), 1178.
28 M. Q. Xie, Y. X. Che, K. Liu, L. X. Jiang, L. M. Xu, R. R. Xue, M. Drechsler, J. B. Huang, B. Z. Tang and Y. Yan, Caking-Inspired Cold Sintering of Plastic Supramolecular Films as Multifunctional Platforms, *Adv. Funct. Mater.*, 2018, **28**(36), 1803370.
29 H. Jin, M. Xie, W. Wang, L. Jiang, W. Chang, Y. Sun, L. Xu, S. Zang, J. Huang and Y. Yan, *et al.*, Pressing-Induced Caking: A General Strategy to Scale-Span Molecular Self-Assembly, *CCS Chem.*, 2020, **2**, 98–106.
30 M. Antonietti, J. Conrad and A. Thuenemann, Polyelectrolyte–Surfactant Complexes: A New Type of Solid, Mesomorphous Material, *Macromolecules*, 1994, **27**(21), 6007.
31 K. Liu, L. Zheng, C. Ma, R. Göstl and A. Herrmann, DNA–surfactant complexes: self-assembly properties and applications, *Chem. Soc. Rev.*, 2017, **46**(16), 5147.
32 T. Kunitake and Y. Okahata, A totally synthetic bilayer membrane, *J. Am. Chem. Soc.*, 1977, **99**(11), 3860.
33 T. Kunitake, Perspectives: Synthetic Bilayer Membrane and Giant Nanomembrane, *Langmuir*, 2016, **32**(47), 12265.

34 P. Batys, Y. Zhang, J. L. Lutkenhaus and M. Sammalkorpi, Hydration and Temperature Response of Water Mobility in Poly(diallyldimethylammonium)–Poly(sodium 4-styrenesulfonate) Complexes, *Macromolecules*, 2018, **51**(20), 8268.

35 M. H. F. Wilkins, A. E. Blaurock and D. M. Engelman, Bilayer Structure in Membranes, *Nature (London), New Biol.*, 1971, **230**(11), 72.

36 J. Rivnay, S. C. B. Mannsfeld, C. E. Miller, A. Salleo and M. F. Toney, Quantitative Determination of Organic Semiconductor Microstructure from the Molecular to Device Scale, *Chem. Rev.*, 2012, **112**(10), 5488.

37 I. C. Khoo, Nonlinear optics of liquid crystalline materials, *Phys. Rep.*, 2009, **471**(5), 221.

38 W. Cui, J. Ji, Y.-F. Cai, H. Li and R. Ran, Robust, anti-fatigue, and self-healing graphene oxide/hydrophobically associated composite hydrogels and their use as recyclable adsorbents for dye wastewater treatment, *J. Mater. Chem. A*, 2015, **3**(33), 17445.

39 R. Das, C. D. Vecitis, A. Schulze, B. Cao, A. F. Ismail, X. Lu, J. Chen and S. Ramakrishna, Recent advances in nanomaterials for water protection and monitoring, *Chem. Soc. Rev.*, 2017, **46**(22), 6946.

40 Y. Yan, W. Xiong, X. Li, T. Lu, J. Huang, Z. Li and H. Fu, Molecular Packing Parameter in Bolaamphiphile Solutions: Adjustment of Aggregate Morphology by Modifying the Solution Conditions, *J. Phys. Chem. B*, 2007, **111**(9), 2225.

